صفحات ۱۰ تا ۱۸

Decoding hand trajectory of ECOG signals using deep learning method

[1]Hanieh Keshtkar
[1] Master's student in Biomedical Engineering at Iran University of Science and Technology

Abstract
This research addresses the significant challenge of limited mobility in individuals affected by limb amputation or spinal cord injuries. The study focuses on Brain-Machine Interface (BMI) systems, which decode neural activities to interpret users' intentions, fostering increased independence in performing tasks. Furthermore, BMI systems hold potential for technological advancements and improving the quality of life for broader populations.

The primary objective is to decode continuous three-dimensional hand position by employing electrocorticography (ECoG) signals recorded from the motor cortex. Notably, the utilization of ECoG signals for estimating hand position in primates is crucial, given their long-term recording capabilities and access to comprehensive datasets. The research incorporates mathematical modeling, feature extraction, and estimation of motor activities based on the analyzed ECoG signals. Challenges include enhancing accuracy and computational efficiency compared to prior investigations. The proposed approach utilizes partial least squares (PLS) regression as the decoding method, demonstrating highly accurate estimation of movements with a notable average correlation coefficient of 0.718, effectively predicting motion trajectories compared to actual measurements.

Keywords
Brain-machine interfaces, ECoG signals, mathematical modeling, partial least squares regression, feature extraction, decoding.

1. Introduction

Initiating a movement and making decisions for complex movements represent the most challenging aspects of motor control. In this process, the frontal cortex plays a fundamental role, and its performance depends on inputs from the cortical region, thalamus, and dopamine system. The motor cortex, a region of the cerebral cortex, is responsible for planning, controlling, and executing voluntary movements. This region is precisely located in front of the central sulcus in the frontal cortex. By recording signals from the motor cortex and interpreting and extracting motor information from them, direct communication between individuals and the external world becomes possible. This is particularly important for patients suffering from spinal cord injuries or severe neurodegenerative diseases, such as ALS, where the ability to move in limbs is compromised, but the brain activity related to these movements persists even years after the onset of disability. Brain-Machine Interface (BMI) systems harness the potential of these brain activities by receiving and interpreting the electrical signals from the brain, thereby generating the necessary control signals for external responses. These responses can include controlling a cursor on a display screen [1],[2],[3], moving prosthetic arms and fingers [4],[5], and even facilitating communication without the need for the individual's own speech system [6],[7]. BMI systems serve as tools that convert the electrical activity generated by neurons in the cortical region into instructions for specific applications, directly used to control external devices. Therefore, they have been considered as means to restore human cognitive or sensory-motor functions. The predominant approach in BMI research has been decoding motor variables based on single-unit activity (SUA) of neurons. Unfortunately, this approach has long-term stability issues and requires daily calibration to maintain reliable performance. To address this problem, Electrocorticography (ECoG) signals can be employed, where the collective neural activity is measured, providing a potentially more durable and stable approach. However, the long-term stability of decoding based on ECoG signals remains uncertain [8]. Due to the proximity of ECoG electrodes to the brain surface, the extracted information from these signals possesses high clarity and accuracy. However, compared to the information recorded within the cortical region that provides neuronal-level resolution, these signals lack high spatial resolution. Nevertheless, these signals provide much of the necessary information for decoding brain activities.

Implanting electrodes directly into the brain, despite its high resolution, has an invasive nature. Therefore, researchers have introduced Electrocorticography (ECoG) where electrodes measure the electrical potential on the cortical surface without penetrating the brain tissue, whether on the pial or subdural surface. Its principles are similar to electroencephalography (EEG) and are also referred to as intracranial EEG. The recording electrodes in the ECoG method, due to their placement on the brain surface, offer higher spatial resolution compared to EEG recording and provide good frequency bandwidth and signal quality. The range of these signals is broader than EEG signals. This capability, coupled with the distance from signal sources such as EMG and EOG, improves the signal-to-noise ratio. The close proximity to the signal source enhances the notable improvement in the spatial resolution of this method [9].

2. Background

ECoG implants were first utilized in the 1950s by Dr. Penfield Wilder and Dr. Jasper Herbert in the well-known Montreal method to locate seizure foci in the brain [9]. Although this recording technique has been clinically used in human patients solely for diagnostic purposes, considering two crucial parameters, electrode placement, and implantation duration, it is rarely employed for research purposes on humans [10]. Nonetheless, researchers have successfully acquired ECoG recordings related to visual and motor information with the consent of patients and demonstrated the capability of this method through offline analysis [11] and [12]. In 2004, the first online ECoG-based brain-machine interface (BMI) for decoding hand movements was investigated [13]. This study involved four participants and focused on controlling a one-dimensional cursor, achieving accuracy ranging from 74% to 100% after a short training period of 3 to 24 minutes. In 2008, another group successfully examined a two-dimensional cursor control system based on imagined or actual motor information [14]. Despite these promising results, current ECoG-BMI studies are limited to a restricted population of epileptic patients for a single training window lasting only a few hours per day [15].

3. Methodology

This project primarily focuses on analyzing ECoG signals. To this end, a dataset provided by the Rekken Institute is utilized. The dataset consists of recordings obtained from contra-lateral cortical activity while a monkey used its hand for food-grasping tasks. Another notable aspect addressed in this section is the presentation of a high-precision model for decoding hand positions using ECoG signals. Various linear and non-linear methods have been proposed for continuous hand decoding using ECoG signals. Linear models are often preferred due to their ease of implementation as they describe the entire movement process using a linear relationship. However, considering the complexity of the underlying brain processes, they may not necessarily be the best choice for modeling. One of the primary challenges of this model is to find the optimal parameters for partial least squares (PLS) regression, leading to improved hand position decoding. Therefore, PLS regression is implemented on this dataset, and the network architecture and training algorithm are fully described.

3.1. Dataset

The dataset used in this study was obtained and shared by the Rekken Institute [16]. This dataset comprises three sessions of recorded electrocorticography (ECoG) from the subdural area beneath the skullcap of a Japanese macaque monkey named K, referred to as sECoG. The array utilized for monkey K consisted of a 64-channel electrode grid implanted in the left hemisphere of the brain, covering the frontal to parietal regions (Figure 1). During each experiment, the monkey was seated facing the experimenter, and its neck was securely held in place by a safety harness. The experimenter presented food morsels at short time intervals in front of the monkey's face, which the monkey received and consumed using its right hand. The monkeys were trained to retrieve the food from the experimenter using their left hand, opposite to the side of the implanted electrode. Each recording session lasted for 15 minutes. A custom jacket with reflective markers was worn by the monkey to capture its movements. These markers were attached to the shoulder, elbow, and wrist of both the left and right hands. Concurrent with the experimental and neural signal recording, hand movements of the monkey were recorded using an optical motion capture system in three-dimensional space. Figure 1 illustrates the position of the electrodes relative to the cortical sulci in monkey K. The cortical sulci are labeled as Ps, Cs, As, and Ips, respectively.

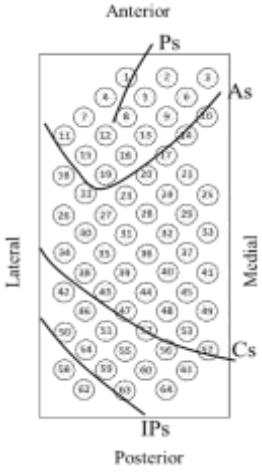

Figure (1): illustrates the positioning of the electrodes relative to the cortical sulci in monkey K [16].

3.2. Preprocessing and Temporal-Frequency Description of ECoG Signals

The ECoG signals were recorded simultaneously with a sampling frequency of 1 kHz, while the hand position was sampled at a frequency of 120 Hz. Initially, the ECoG signals were passed through a bandpass filter with a range of 0.1 to 600 Hz. Subsequently, the difference between the signal obtained from each channel at any given moment in time and the momentary average of the recorded signals for all channels was determined. This method, known as Common Average Reference (CAR), is a simple and effective approach for removing common noise across all channels [17]. Equation (1) illustrates the process by which this method is applied, where $x_i\ (t)$ represents the raw recorded signal from channel i , and $x_i^{CAR}(t)$ represents the noise-reduced signal using the CAR method.

(1) $x_{ch}^{CAR}(t) = x_{ch}(t) - \sum_{n=1}^{64} x_n(t)\,; \quad ch = 1{:}64$

The motion tracker markers were sampled at a frequency of 20 Hz because the position data, which contained movement information, showed negligible variance in frequencies above 15 Hz. The three-dimensional hand trajectories were based on coordinates with the origin precisely at the midpoint between the two shoulders (X: left-right, Y: front-back, Z: up-down), where the X-axis aligns with the shoulders. The obtained coordinates were then normalized using z-score. To extract features from the time-frequency representation (spectrogram), the Morlet wavelet transform was employed. For each channel, 10 central frequencies were created ranging from 10 Hz to 150 Hz. To create the time dimension of the spectrogram for each channel, time windows of 1.1 seconds with a step size of 50 milliseconds were used. As illustrated in Figure 2, the spectrogram was generated from t -1.1 to t to achieve a time-frequency representation of 1100 × 10 (Figure 2-a). To reduce the dimensionality of the feature matrix, a sampling rate of 100 milliseconds was applied to the time dimension, resulting in a 10 × 10 spectrogram matrix (Figure 2-b). Finally, each of the 10 frequencies was normalized using z-score over time (Figure 2-c). Thus, the preprocessed ECoG data were prepared for decoding movement information.

3.3. Decoding Method

The main objective of this research is to decode motion information using the PLS regression method. Therefore, the focus has been on finding the optimal transformation component. The parameter settings were carefully determined through extensive trial and error, considering the most favorable configuration for each parameter. The decoding method discussed here is designed to maximize the correlation coefficient between the actual hand movement trajectory and the predicted trajectory for the dataset used in this study.

3.3.1. PLS Method

The method investigated in this research is the PLS method, which has recently gained attention in various studies due to its satisfactory accuracy [18]. In this study, PLS is utilized for decoding the hand motion pattern. The weaknesses and challenges associated with other regression methods have been overcome in this approach, as detailed below.

PLS is a supervised feature extraction method that linearly transforms a low-level feature vector $\mathbf{u} \in R^{1\times m}$ into a lower-dimensional vector $\mathbf{x} \in R^{1\times l}$ by reducing the shared information among the extracted features. Moreover, the maximum information relevant to the target, which is the supervisor used in training the PLS model, will be present in the new features.

If we denote the low-level feature matrix as $\mathbf{X} \in R^{n\times m}$ and the target matrix as $\mathbf{Y} \in R^{n\times p}$, where in these equations, n represents the number of training samples, m denotes the dimensionality of the low-level feature vector, and p represents the dimensionality of the target vector (i.e., the label used for supervised feature extraction). In the PLS transformation, these two matrices are decomposed in a way that maximizes the correlation between the projected components of these two matrices.

$$\boldsymbol{X} = \mathbf{P}_X \times \mathbf{T}_X{}^T + \mathbf{E} \quad (2)$$

$$\boldsymbol{Y} = \mathbf{Q}_Y \times \mathbf{U}_Y{}^T + \mathbf{F} \quad (3)$$

$$\mathbf{x} = \mathbf{u} \times (\mathbf{P}_X \mathbf{P}_X^T)^{-1} \mathbf{P}_X \quad (4)$$

In equations (2) and (3), $\mathbf{T}_X \in R^{n\times l}$ and $\mathbf{U}_Y \in R^{n\times l}$ (referred to as scores) are obtained by projecting matrices $\boldsymbol{X}$ and $\boldsymbol{Y}$ onto matrices $\mathbf{P}_X \in R^{m\times l}$ and $\mathbf{Q}_Y \in R^{p\times l}$ (referred to as loadings), respectively. Moreover, "**E**" and "**F**" represent the error values in this decomposition. This decomposition should be performed in such a way that the projected matrices, namely $\mathbf{T}_X$ and $\mathbf{U}_Y$, exhibit the highest correlation with each other. NIPALS and SIMPLS [19] are two commonly used methods for calculating PLS, and in this study, pre-existing MATLAB library codes based on the SIMPLS method were utilized. The SIMPLS method is faster and simpler compared to NIPALS. Once $\mathbf{P}_X$ is computed using the training samples, the PLS components, denoted as $\mathbf{x} \in R^{1\times l}$, are calculated using equation (4) for a given low-level feature vector $\mathbf{u} \in R^{1\times m}$ [20], [18].

In this study, the extracted vector "x", which represents the image of the vector "u" in the PLS space, has been employed as the feature vector. To determine the optimal PLS transformation order (i.e., "l"), a 10-fold cross-validation strategy has been applied to the training dataset. This involved dividing the training dataset into 10 equal parts, where 9 parts were used for training the linear model, and the remaining part was used for testing the model and estimating the results. For each of these 10 different scenarios, the value of "l" varied from 1 to a specified value (chosen as 100 in this study), and the training and result estimation process was repeated. In the next step, the average value of these results across all 10 different scenarios was calculated to ultimately select the value of "l" as the order of the extracted features that yields the best decoding results based on the minimum estimation error.

Figure (3) illustrates an example of the computed curve depicting the relationship between the number of PLS latent components and decoding estimation error. The horizontal axis represents the dimensions of the extracted feature vector, while the vertical axis represents the decoding estimation error between the estimated position and the actual position of the hand in relation to the mentioned feature vector. This averaging across the 10 obtained results using the 10-fold cross-validation method was performed. As evident from this figure, the best result for the given sample is achieved for $l = 15$.

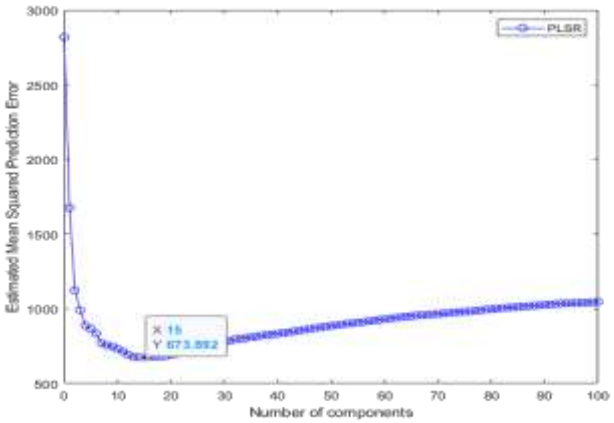

Figure (3): depicts a curve illustrating the relationship between the number of extracted feature components and the prediction error. The optimal decoding result is achieved when the number of components yields the minimum estimation error.

3.4. Evaluation Criteria

In order to quantitatively assess the significance of the obtained results, two evaluation criteria have been utilized in this study. To measure the accuracy of estimating the hand's trajectory, the correlation between the actual and estimated hand trajectories has been calculated. This criterion, denoted as "r" and computed according to Equation (5), takes values smaller than or equal to 1. As the correlation approaches 1, it indicates the highest similarity, while values deviating from 1 indicate lower similarity.

The second criterion employed in this study is the root mean square of the normalized error (RMSE). Based on this criterion, a higher similarity between the actual and estimated trajectories leads to a value closer to zero, while a lower similarity results in a value closer to 1. Equation (6) illustrates the calculation method for this evaluation criterion.

These evaluation criteria have been utilized to assess the importance and quality of the obtained results in a quantitative manner.

$$r = \frac{\sum_{t=1}^{T}(y(t)-\bar{y})(y_d(t)-\bar{y}_d)}{\sqrt{\sum_{t=1}^{T}(y(t)-\bar{y})^2(y_d(t)-\bar{y}_d)^2}} \quad (5)$$

$$RMSE = \sqrt{\frac{1}{T}\sum_{t=1}^{T}(y(t)-y_d(t))^2} \quad (6)$$

In these equations, $y(t)$ and $y_d(t)$ represent the estimated and actual hand positions, respectively, at time sample t. Furthermore, $\bar{y}$ and $\bar{y}_d$ denote the average estimated and actual hand positions over T time samples.

4. Results and Discussion

This section examines the roles of different regions of the brain cortex in motion control and identifies the region with the most motion-related information. This analysis greatly aids the decoding process by reducing computation time. Subsequently, using Partial Least Squares (PLS), the decoding of wrist, elbow, and shoulder positions in three dimensions (X, Y, and Z) is performed for the right hand.

4.1. Results Obtained from the PLS Model

After training the PLS model on the training dataset, its performance is evaluated using the test data. The available dataset consists of three recording sessions. Table (1) presents the decoding results for the wrist, elbow, and shoulder positions in three dimensions (X, Y, and Z) for each session. The average correlation coefficient (r) for all sessions using the PLS decoding model is calculated to be 0.72, with an average RMSE of 0.20.

Table (1): displays the motion decoding results for the right hand of monkey K using the PLS method. The model is evaluated based on two parameters: correlation coefficient (r) and root mean square error (RMSE).

Location of the markers		Session 1		Session 2		Session 3		Mean	
		r	RMSE	r	RMSE	r	RMSE	r	RMSE
RWRI	X	0.517	0.190	0.227	0.181	0.618	0.250	0.454±0.11	0.207±0.02
	Y	0.722	0.247	0.768	0.200	0.694	0.391	0.728±0.02	0.279±0.05
	Z	0.859	0.271	0.847	0.238	0.852	0.356	0.853±0.003	0.288±0.03
RELB	X	0.716	0.082	0.544	0.080	0.792	0.136	0.684±0.07	0.099±0.01
	Y	0.781	0.221	0.836	0.184	0.825	0.272	0.814±0.01	0.225±0.02
	Z	0.779	0.129	0.781	0.155	0.855	0.207	0.805±0.02	0.163±0.02
RSHO	X	0.785	0.036	0.602	0.040	0.503	0.042	0.630±0.08	0.039±0.001
	Y	0.698	0.107	0.799	0.063	0.719	0.114	0.739±0.03	0.094±0.01
	Z	0.720	0.069	0.701	0.688	0.852	0.606	0.758±0.04	0.454±0.19
TOTAL AVERAGE			r				0.718±0.02		
			RMSE				0.205±0.03		

The presented model demonstrates satisfactory performance in decrypting the trajectory of the hand's elbow motion compared to the wrist and shoulder. Since the wrist position represents the complete path to the target, it is considered the primary comparison criterion. The decoding accuracy of the right hand's elbow trajectory in the X, Y, and Z directions is obtained as 0.45, 0.72, and 0.85, respectively, indicating that the model achieves a higher correlation coefficient along the Z-axis. Additionally, the RMSE values for the right hand's elbow in the X, Y, and Z directions are calculated as 0.21, 0.28, and 0.29, respectively, indicating higher error in the Z dimension. Despite the satisfactory results and high accuracy of this approach, its practical implementation for large-scale datasets is challenging due to the extremely high computational time (over five hours for a single hand).

Figure (4) illustrates an example of decrypting the trajectory of the right hand's elbow motion using PLS. In this figure, the blue line represents the actual motion path, while the red line represents the predicted motion path. The correlation coefficients for the X, Y, and Z dimensions are 0.61, 0.69, and 0.85, respectively.

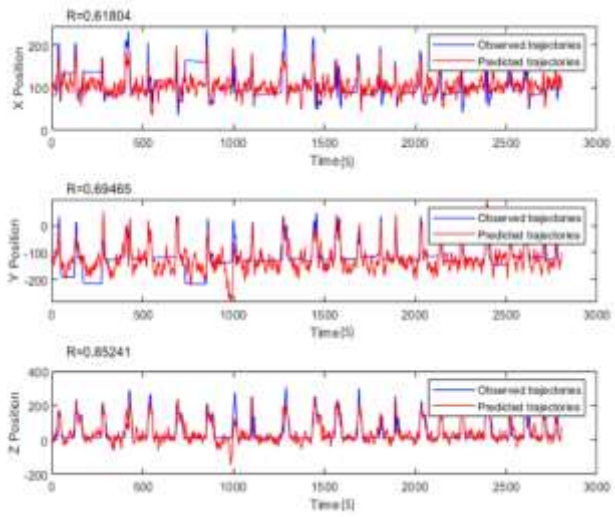

Figure (4) illustrates a sample of decoding the three-dimensional wrist position using PLS. The number of components is set to 14. The blue path represents the actual motion trajectory, while the red path represents the predicted motion trajectory. The correlation coefficients for the X, Y, and Z dimensions are 0.61, 0.69, and 0.85, respectively.

4.2. Decoding Motor and Somatosensory Cortical Information

The selection of different brain regions for decoding motor-related information has always been a challenge for researchers aiming to improve results. In this study, to address the computational time issue in the PLS model, a proposed approach involves excluding channels with minimal motor-related information. Consequently, the crucial and influential roles of the primary motor cortex (M1) and primary somatosensory cortex (S1) in motor control have been investigated.

4.2.1. Channel Selection

As depicted in Figure 5, regions M1 and S1 are located on both sides of the central sulcus (Figure 5a). Referring to the arrangement of the ECoG electrode array beneath the skull, channels corresponding to M1 and S1 are individually selected for decoding. This enables the identification of brain regions that contain richer motor-related information. By increasing their influence and eliminating channels with lesser motor information, the decoding methods can improve the speed and accuracy of decoding.

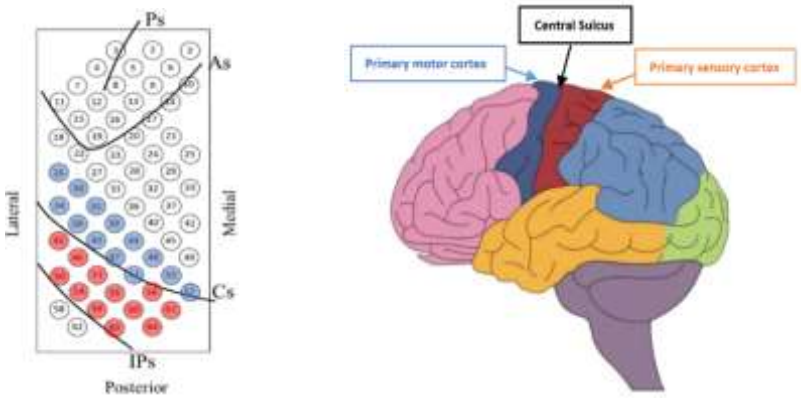

(a) (b)

Figure (5): displays the precise location of M1 and S1 regions relative to the brain sulci. (a) The central sulcus is situated between the M1 and S1 regions [19]. (b) The electrode array placement on the left hemisphere of the monkey brain is depicted. The 64-channel electrode array covers the area from the frontal to the parietal region. The channels marked in blue correspond to the M1 region, while the channels in pink represent the S1 region.

4.2.2. Decoding the S1 Region

As shown in Figure 5b, the pink-colored channels have been selected as the S1 region. Table 2 presents the results of decoding the right-hand wrist position, with decoding accuracy calculated for the X, Y, and Z dimensions as 0.37, 0.65, and 0.81, respectively. Although there was a slight decrease in decoding accuracy, the computational time reduced to approximately one-sixth of the total channel processing time.

Table (2): presents the decoding of the wrist motion trajectory for the S1 region in monkey K using the PLS method. The model was evaluated using two performance parameters: correlation coefficient (r) and root mean square error (RMSE).

Location of the markers		Session 1		Session 2		Session 3		Mean	
		r	RMSE	r	RMSE	r	RMSE	r	RMSE
RWRI	X	0.468	0.191	0.139	0.196	0.496	0.283	0.367±0.11	0.223±0.02
	Y	0.643	0.272	0.653	0.253	0.645	0.417	0.647±0.003	0.314±0.05
	Z	0.802	0.311	0.820	0.309	0.800	0.406	0.807±0.006	0.342±0.03
TOTAL AVERAGE		r						0.607±0.07	
		RMSE						0.293±0.02	

4.2.3. Decoding the M1 Region

As shown in Figure 5b, the blue-colored channels have been selected as the M1 region and used for decoding in the model. The results obtained from this region are indicated in Table 3. These results demonstrate the crucial role of the M1 region in motor control within the cortical brain area, emphasizing its significance for decoding motor information. By decoding information specifically from this region, researchers are enabled to achieve the desired accuracy without decoding all the channels. Table 3 presents the results of decoding the right-hand wrist position, with decoding accuracy for the X, Y, and Z dimensions being 0.39, 0.75, and 0.87, respectively. By comparing these results to the case where all channels were used for decoding, it becomes evident that despite the decrease in accuracy in the X dimension, the decoding accuracy has increased in the other two dimensions. Consequently, not only the computational time issue has been resolved, but the overall accuracy of the model has also improved to some extent.

Table (3): presents the decoding of the wrist motion trajectory for the M1 region in monkey K using the PLS method. The model was evaluated using two performance parameters: correlation coefficient (r) and root mean square error (RMSE).

Location of the markers		Session 1		Session 2		Session 3		Mean	
		r	RMSE	r	RMSE	r	RMSE	r	RMSE
RWRI	X	0.437	0.196	0.208	0.191	0.517	0.274	0.387±0.09	0.220±0.02
	Y	0.767	0.227	0.770	0.211	0.714	0.367	0.750±0.01	0.268±0.04
	Z	0.859	0.271	0.896	0.234	0.871	0.331	0.875±0.01	0.278±0.02
TOTAL AVERAGE		r						0.671±0.07	
		RMSE						0.255±0.02	

4.3. Comparison of PLS Method Performance in the Three Axes of X, Y, and Z Movement Separately

To provide a better comparison, the results have been calculated separately for each movement axis in terms of the average r and RMSE According to Table 4, the average correlation coefficient for the proposed model was lower in the X axis compared to the Y and Z axes ($P < 0.01$). As shown in Table 4, the parameter r for the PLS method estimated the correlation between the predicted trajectory and the actual wrist motion trajectory to be 0.60, 0.76, and 0.81 for the X, Y, and Z axes, respectively, indicating a considerable level of accuracy.

4.4. Comparison of PLS Method Performance in Predicting Trajectories of Right Hand's Wrist, Elbow, and Shoulder

One of the significant advantages of this research is the simultaneous recording of movements in the right hand's wrist, elbow, and shoulder. By predicting the trajectory of movement in all three regions, the model's decoding capability in terms of positional indicators has been enhanced. According to Table 5, after decoding the motion information by the proposed model, the values of two evaluation parameters, namely, r and RMSE, have been estimated for all three parts of the right hand. It is evident

that the correlation coefficient between the predicted and actual motion trajectory has slightly decreased for the wrist compared to the shoulder and elbow. Through variance analysis, it was determined that the proposed method had better decoding performance in predicting the trajectory of elbow movements in the right hand.

5. Conclusion

In this study, we presented the results of estimating hand position using the proposed model, which is based on partial least squares (PLS) regression. The decoding capability of this method was evaluated separately for each axis and position using the r and RMSE parameters. The decoding results of motion information using the PLS method yielded an average correlation coefficient of 0.718±0.02 and an RMSE of 0.205±0.03. These results indicate the high accuracy of the proposed model.

Despite the satisfactory accuracy of the PLS method, it is important to note that the performance of BMI systems and the improvement of degrees of freedom in prosthetic limbs benefit from increased decoding accuracy.

Based on our study, the following recommendations are proposed for future research:

1. Investigate the performance of alternative decoding methods, such as deep neural networks, to further improve the accuracy of decoding motion information.

2. Explore the use of frequency-pass filters specific to brain waves for BMI systems, which can enhance the decoding performance.

3. Conduct comparative studies between the PLS method and other regression techniques to assess their respective advantages and limitations in decoding hand motion.

4. Expand the study to include a larger dataset and a more diverse range of hand motions to validate the generalizability of the proposed model.

By addressing these recommendations, future research can contribute to the advancement of decoding techniques and the development of more accurate and robust systems for BMI and prosthetic limb control.

6. References

[1] *S. Kim, J. D. Simeral, L. R. Hochberg, J. P. Donoghue and M. J. Black, "Neural control of computer cursor velocity by decoding motor cortical spiking activity in human with tetraplegia," J. Neural Eng., vol. 5, pp. 455-476, 2008.*

[2] *S. Kim, J. D. Simeral, L. R. Hochberg, J. P. Donoghue, G. M. Friehs and M. J. Black, "Point and click cursor control with an intracortical neural interface system by humans with tetraplegia,," S.P. Kim, J.D. Simeral, L.R. Hochberg, J.P. Donoghue, G.M. Friehs, and M.J. Black, "Point and click cursor control with an intracortical neural IEEE transactions on neural systems and rehabilitation engineering, vol. 19, pp. 193-203, April 2011.*

[3] *L. Hochberg, M. D. Serruya, G. M. Friehs, J. A. Mukand, M. Saleh, A. H. Caplan, A. Branner, D. Chen, R. D. Penn and J. P. Donoghue, "Neuronal ensemble control of prosthetic devices by a human with tetraplegia," nature, vol. 442, pp. 164-171, July 2016.*

[4] *J. Zhuang, W. Truccolo, I. C. V and J. P. Donoghue, "Decoding 3-D reach and grasp kinematics from high-frequency local field potentials in primate primary motor cortex,," IEEE transactions on biomedical engineering, vol. 57, pp. 1774-1784, July 2010.*

[5] *M. Velliste, S. Perel, M. Spalding, A. S. Whitford and A. B. Schwartz, "Cortical control of a prosthetic arm for self-feeding,," nature, vol. 453, pp. 214-225, June 2008.*

[6] *V. Kanas, I. Mporas, H. Benz, K. N. Sgarbas, A. Bezerianos and N. E. Crone, "Joint spatial-spectral feature space clustering for speech activity detection from ECoG signals," IEEE Transactions on Biomedical Engineering,, vol. 61, no. 4, pp. 1241-1250, 2014.*

[7] *B. Pasley, S. David, N. Mesgarani and et.al, "Reconstructing speech from human auditory cortex," PloS Biology, vol. 10, January 2012.*

[8] *S. Grillner and A. El Manira, "CURRENT PRINCIPLES OF MOTOR CONTROL, WITH SPECIAL REFERENCE TO VERTEBRATE LOCOMOTION," Physiol Rev, pp. 271-320, First published September 12, 2019, 2020.*

[9] *G. Schalk and E. C. Leuthardt, "Brain-computer interfaces using electrocorticographic signals," IEEE review in biomedical engineering, vol. 04, pp. 140-154, October 2011.*

[10] *E. Sutter, "The brain response interface: communication through visually-induced electrical brain responses," Journal of Microcomputer Applications, vol. 15, no. 01, pp. 31-45, 1992.*

[11] *N. Crone, D. L. Miglioretti, B. Gordon and R. P. Lesser, "Functional mapping of human sensorimotor cortex with electrocorticographic spectral analysis. I. Alpha and beta event-related desynchronization.," 1998.*

[12] *N. E. Crone, D. L. Miglioretti, B. Gordon and R. P. Lesser, "Functional mapping of human sensorimotor cortex with electrocorticographic spectral analysis. II. Event-related synchronization in the gamma band," Brain, vol. 121, pp. 2301-2315, 1998.*

[13] *E. Leuthardt, G. Schalk, J. R. Wolpaw, J. G. Ojemann and D. W. Moran, "A brain-computer interface using electrocorticographic signals in humans," 2004.*

[14] *G. Schalk, K. J. Miller, N. R. Anderson, J. A. Wilson, M. D. Smyth, J. G. Ojemann, D. W. Moran, J. R. Wolpaw and E. C. Leuthardt, "Two-dimensional movement control using electrocorticographic signals in humans," J. Neural Eng, vol. 5, no. 1, pp. 75-84, 2008.*

[15] *W. J. Freeman, L. J. Rogers, M. D. Holmes and D. L. Silbergeld, "Spatial spectral analysis of human electrocorticograms including the alpha and gamma bands," J. Neurosci. Methods,, vol. 95, no. 2, pp. 111-121, 2000.*

[16] *Z. C. Chao, Y. Nagasaka and N. Fujii, "Long-term asynchronous decoding of arm motion using electrocorticographic signals in monkeys," Frontiers in Neuroengineering, vol. 3, 30 March 2010.*

[17] *R. Foodeh, A. Khorasani, V. Shalchyan and M. R. Daliri, "Minimum noise estimate filter: a novel automated artifacts removal method for field potentials," IEEE Trans. Neural Syst. Rehabil. Eng., vol. 25, no. 8, pp. 1143-1152, 2017.*

[18] *B. Farrokhi and A. Erfanian, "A state-based probabilistic method for decoding hand position during movement from ECoG signals in non-human primate," 2020.*

[19] *S. de Jong, "SIMPLS: An alternative approach to partial least squares regression," Chemom. Intell. Lab. Syst., vol. 18, no. 3, pp. 251-263, 1993.*

[20] *S. Wold, M. Sjöström and L. Eriksson, "PLS-regression: a basic tool of chemometrics," Chemometrics and Intelligent Laboratory Systems, vol. 58, pp. 109-130, 2001.*